Supporting Information for:

Towards Automated Free Energy Calculation with Accelerated Enveloping Distribution Sampling (A-EDS)

Jan Walther Perthold, Dražen Petrov, Chris Oostenbrink*

Institute for Molecular Modeling and Simulation, Department for Material Sciences and Process Engineering, University of Natural Resources and Life Sciences (BOKU), Vienna, Muthgasse 18, 1190 Vienna, Austria

Corresponding Author

*E-mail: chris.oostenbrink@boku.ac.at

Table S1. Definition of the harmonic protein-ligand distance restraint for system TRP.

Protein atom	Ligand atom	Distance [nm]	Force constant [kJ·mol^{-1}·nm^{-2}]
ASP171 Cγ	Cε	0.42	250

Table S2. Definition of harmonic protein-ligand distance restraints for system PNMT.

Protein atom(s) (COM)	Ligand atoms (COM)	Distance [nm]	Force constant [kJ·mol^{-1}·nm^{-2}]
PHE161 Cδ1, Cδ2, Cε1, Cε2	Cα, Cβ, Cδ, Cε	0.38	250
TYR64 Cδ1, Cδ2, Cε1, Cε2	Cα, Cβ, Cδ, Cε	0.83	250
VAL32 Cβ	Cα, Cβ, Cδ, Cε	0.72	250

Table S3. Computed binding affinities for GRA2 ligands and comparison to experimental data and results obtained with different methods. Energy units are kJ·mol^{-1}.

Ligand	A-EDS (2σ)	A-EDS (3σ)	Experiment[1]	TI[1]	OSP[1]	A-EDS ($\Delta E_{max}^*=100$)[2]
1	-27.4	-28.0	-30.8	-31.9	-32.1	-30.6
2	-29.8	-37.8	-36.8	-34.4	-37.0	-39.4
3	-26.9	-33.3	-31.7	-27.2	-30.7	-34.2
4	-37.3	-20.5	-29.4	-28.5	-32.0	-26.8
5	-35.3	-37.3	-28.0	-34.8	-25.1	-25.7
6	-33.1	-43.6	n.a.	n.a.	-31.8	n.a.
7	-35.9	-26.0	n.a.	n.a.	-34.3	n.a.
8	-45.5	-48.9	n.a.	n.a.	-22.5	n.a.
9	-39.6	-24.1	n.a.	n.a.	-29.3	n.a.
10	-43.2	-41.3	n.a.	n.a.	-22.7	n.a.
11	-48.6	-25.9	n.a.	n.a.	-19.3	n.a.
12	-40.9	-31.6	n.a.	n.a.	-29.6	n.a.
13	-53.6	-52.8	n.a.	n.a.	-21.4	n.a.
14	-51.1	-35.4	n.a.	n.a.	-14.0	n.a.
15	-54.3	-31.7	n.a.	n.a.	-18.9	n.a.
16	-58.7	-41.6	n.a.	n.a.	-7.5	n.a.
RMSE to experiment	6.3	6.0		3.9	1.9	2.2

Table S4. Computed binding affinities for TRP ligands and comparison to experimental data and results obtained with different methods. Energy units are kJ·mol^{-1}.

Ligand	A-EDS (1σ)	A-EDS (2σ)	A-EDS (3σ)	Experiment[3]	TI[4]	OSP/TPF[4]
1	-29.1	-28.5	-28.6	-26.5	-23.1	-24.7
2	-19.5	-13.6	-27.8	-20.5	-32.4	-23.3
3	-24.4	-22.6	-18.4	-28.1	-21.0	-25.2
4	-31.2	-32.2	-36.3	-20.2	-28.3	-25.6
5	-16.5	-23.8	-20.9	-26.9	-22.7	-26.5
6	-28.0	-28.8	-22.9	-25.3	-23.0	-23.2
7	-21.8	-21.5	-16.2	-23.3	-20.0	-22.1
8	-4.3	-3.8	6.4	n.a.	14.5	20.0
RMSE to experiment	6.1	6.0	8.5		6.6	2.8

n.a.: not available

Table S5. Computed binding affinities for PNMT ligands and comparison to experimental data and results obtained with different methods. Energy units are kJ·mol^{-1}.

Ligand	A-EDS (2σ)	A-EDS (3σ)	Experiment[5-10]	TI[5]	EDS[11]	RE-EDS[12]
1	-21.2	-26.7	-30.1	-30.0	-23.6	-26.5
2	201.2	196.5	> -15.5[a,b]	48.9	n.a.	n.a.
3	-26.2	-28.6	-25.4[b]	-25.7	-23.8	-28.1
4	-35.2	-30.4	-26.6[a,b]	-31.1	-24.3	-29.4
5	-31.1	-37.2	-40.9	-39.7	-35.9	-36.8
6	-42.9	-31.7	-34.8	-40.3	-45.2	-32.4
7	-23.6	-41.2	-39.8	-41.5	-35.5	-39.3
8	-49.9	-36.3	-41.9[c]	-42.9	-43.0	-39.1
9	-35.6	-34.9	-33.9[b]	-29.0	-35.9	-34.8
10	-31.3	-30.2	-24.0[a,b]	-17.4	-29.9	-30.7
RMSE to experiment	8.8	3.8		3.7	5.2	4.9

[a]experimental data refers to racemic mixture

[b]experimental data refers to binding to bovine PNMT

[c]experimental data refers to other enantiomer
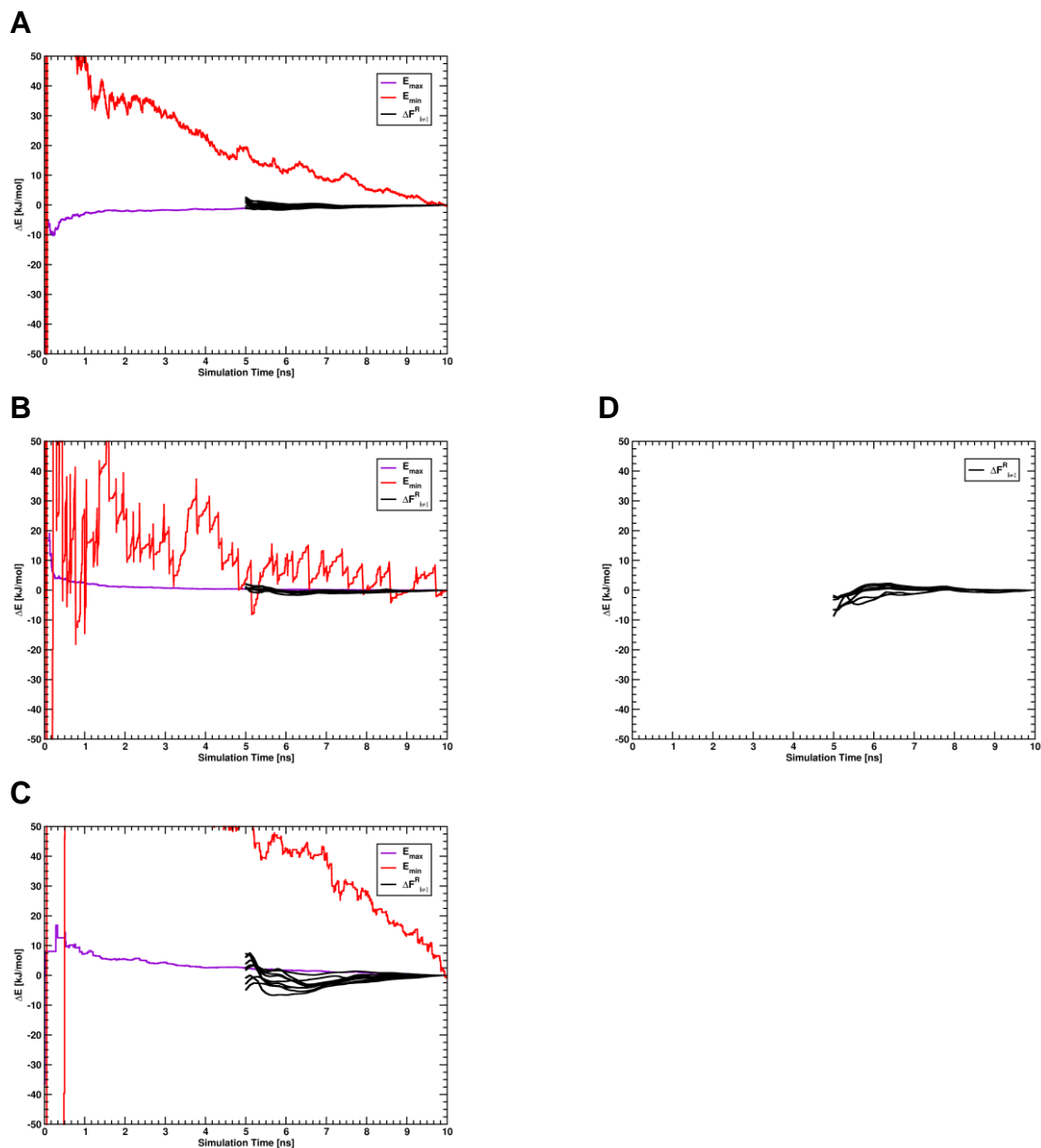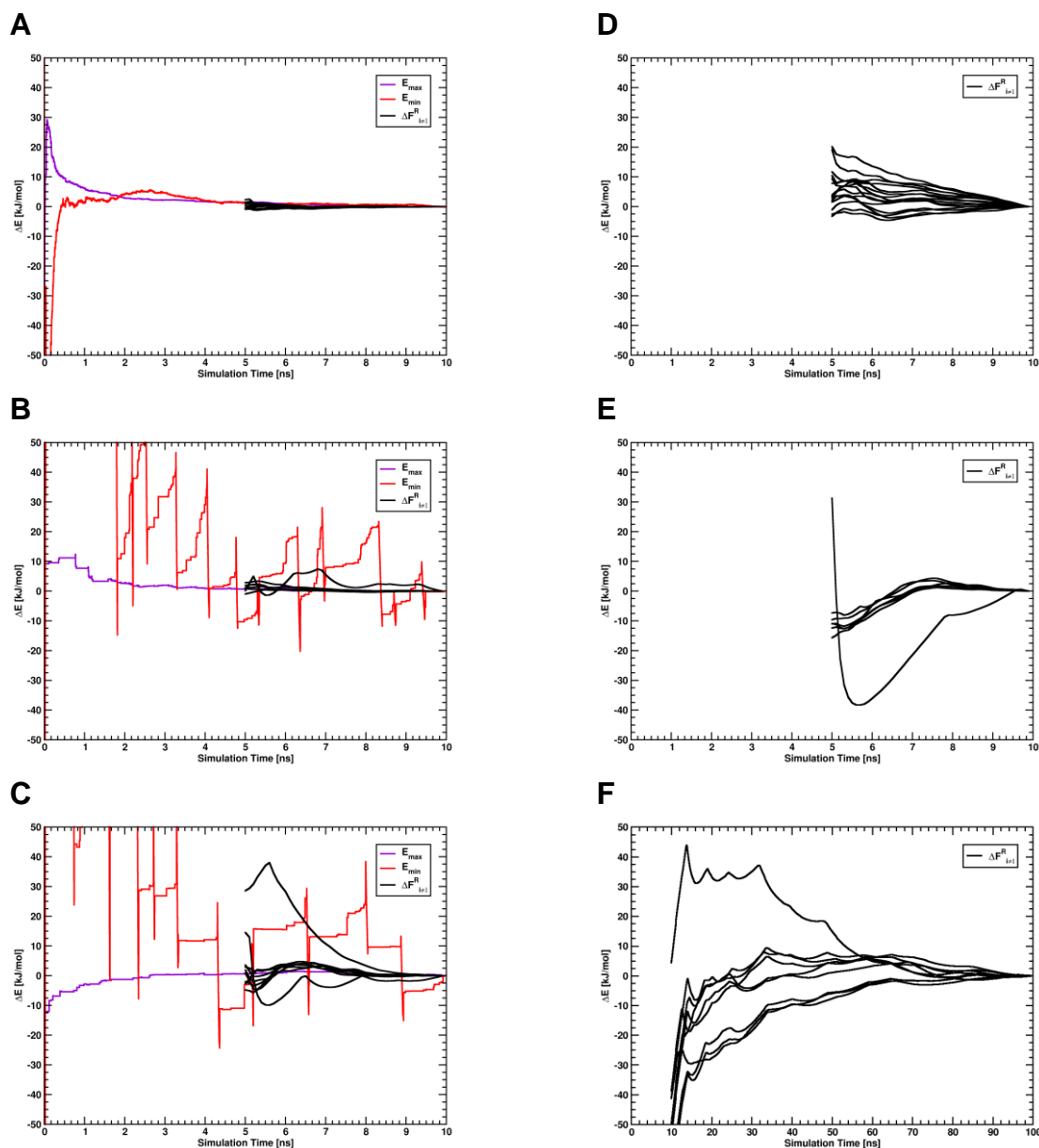
n.a.: not available

Figure S1. Convergence of the A-EDS acceleration parameters E_{max} and E_{min} and the free-energy offset parameters $\Delta F_{i\neq1}^{R}$ relative to their final values for the A-EDS parameter search simulation with an acceleration σ-level of 1σ, for the unbound ligands in water of system GRA2 (A), TRP (B) and PNMT (C), and for the ligands bound to the protein of system TRP (D). The convergence of the free-energy offset parameters $\Delta F_{i\neq1}^{R}$ is shown as forward cumulative average over the free-energy offset trajectory from which the first 5 ns were discarded as non-equilibrated region. Note that in panels A, B and C the A-EDS parameter E_{min} (red solid line) falls off the plot in the first half of the trajectory.

Figure S2. Convergence of the A-EDS acceleration parameters E_{max} and E_{min} and the free-energy offset parameters $\Delta F_{i\neq1}^R$ relative to their final values for the A-EDS parameter search simulation with an acceleration σ-level of 3σ, for the unbound ligands in water of system GRA2 (A), TRP (B) and PNMT (C), and for the ligands bound to the protein of system GRA2 (D), TRP (E) and PNMT (F). The convergence of the free-energy offset parameters $\Delta F_{i\neq1}^R$ is shown as forward cumulative average over the free-energy offset trajectory from which the first 5 or 10 ns were discarded as non-equilibrated region. Note that in panels A, B and C the A-EDS parameter E_{min} (red solid line) falls off the plot in the first half of the trajectory.
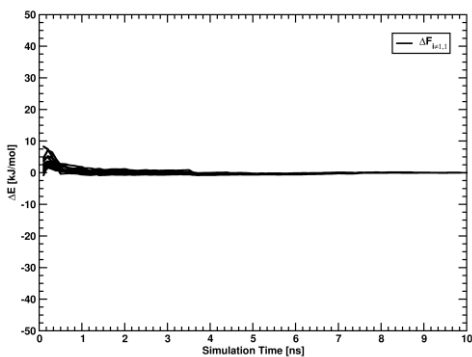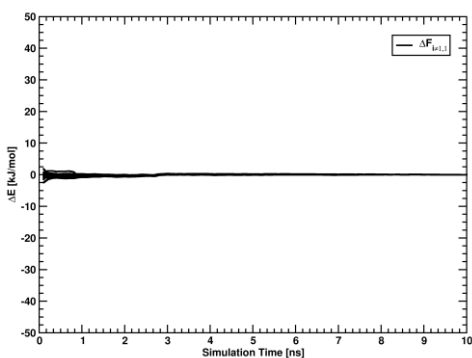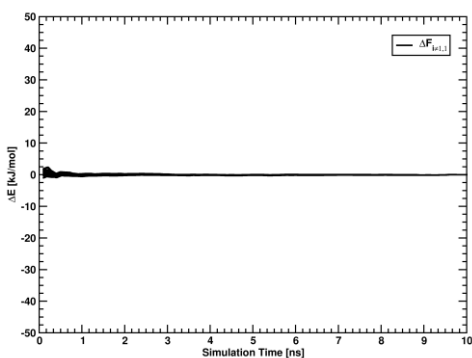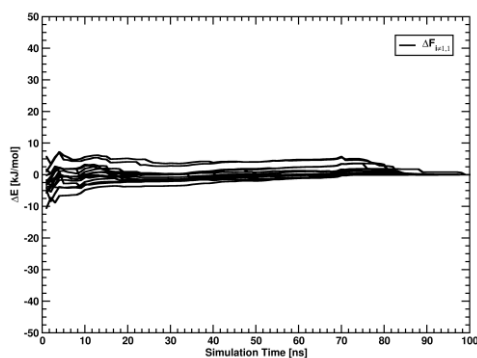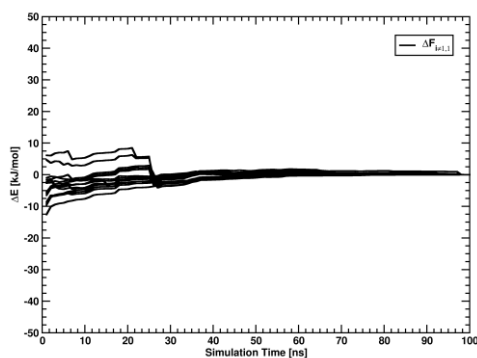
Figure S3. Convergence of the calculated relative free-energy differences $\Delta F_{i\neq 1,1}$ between the ligand end-states relative to their final values from the equilibrium A-EDS simulations of the unbound reference-state ligand in water for acceleration σ-levels of 1σ (A), 2σ (B) and 3σ (C), and for the reference-state ligand bound to the protein for acceleration σ-levels of 2σ (D) and 3σ (E) of system GRA2.
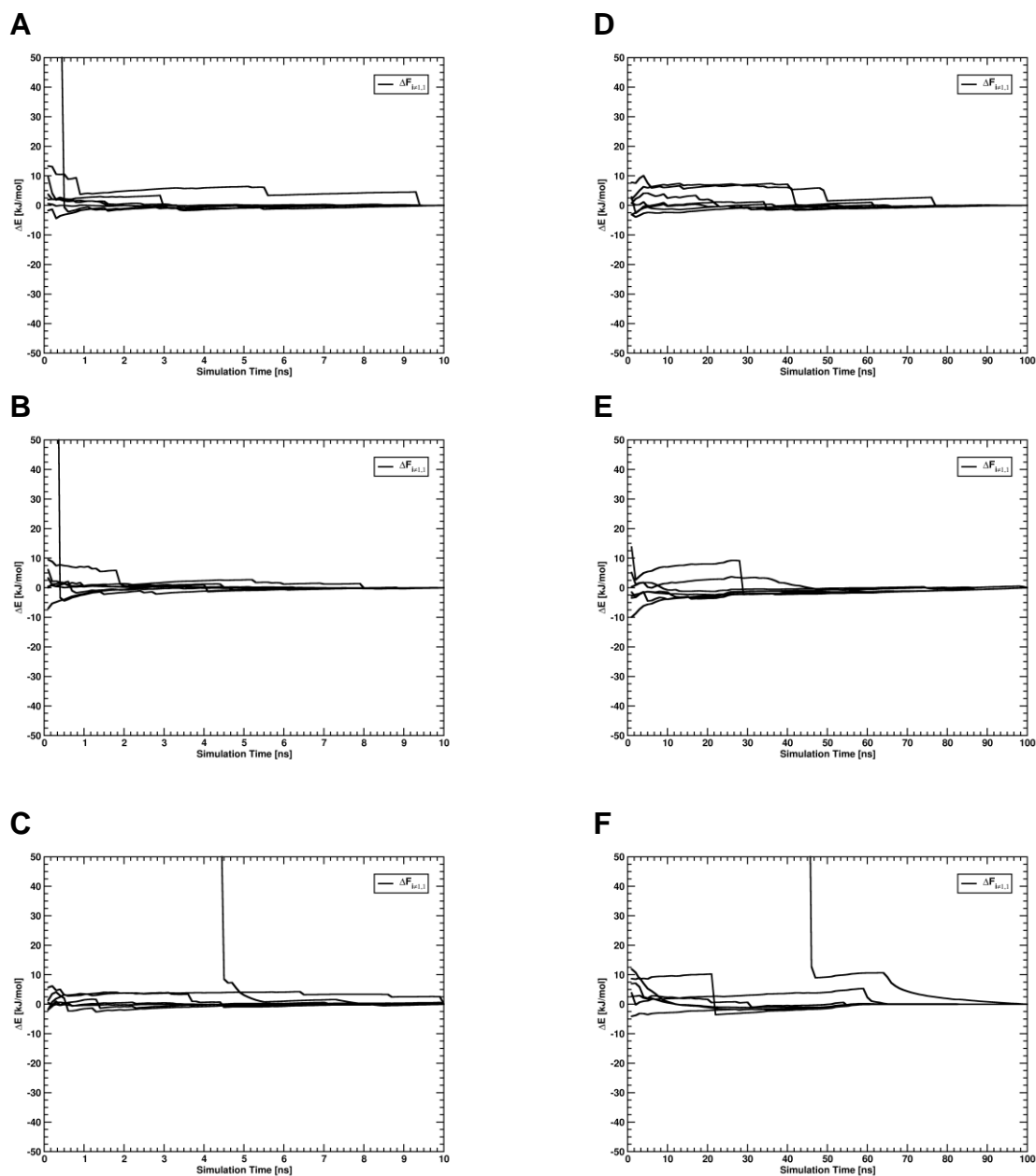
Figure S4. Convergence of the calculated relative free-energy differences $\Delta F_{i \neq 1,1}$ between the ligand end-states relative to their final values from the equilibrium A-EDS simulations of the unbound reference-state ligand in water for acceleration σ-levels of 1σ (A), 2σ (B) and 3σ (C), and for the reference-state ligand bound to the protein for acceleration σ-levels of 1σ (D), 2σ (E) and 3σ (F) of system TRP. Note that in panels C and F one relative free-energy difference $\Delta F_{i \neq 1,1}$ falls off the plot in the first half of the trajectory.
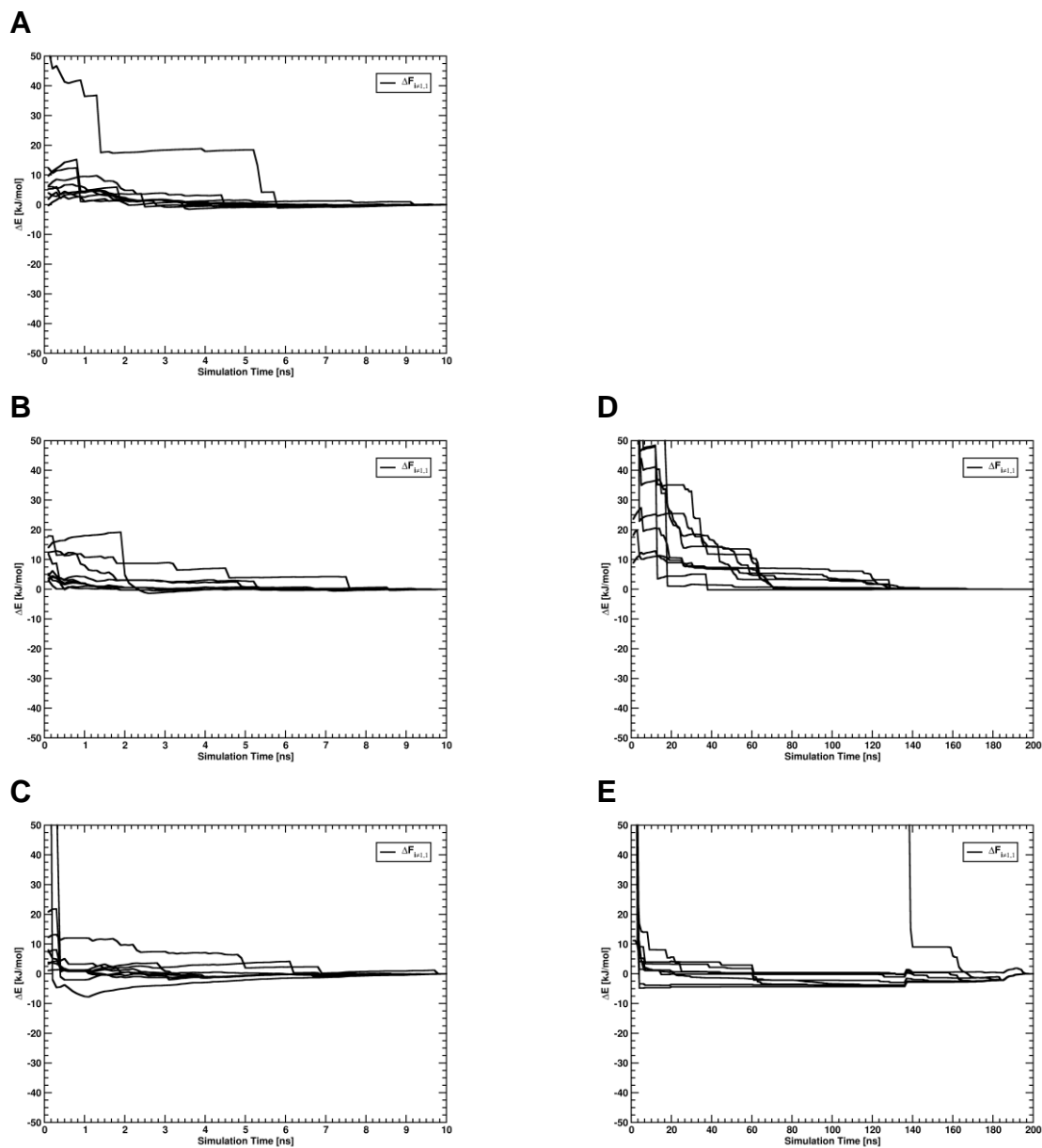
Figure S5. Convergence of the calculated relative free-energy differences $\Delta F_{i\neq1,1}$ between the ligand end-states to relative their final values from the equilibrium A-EDS simulations of the unbound reference-state ligand in water for acceleration σ-levels of 1σ (A), 2σ (B) and 3σ (C), and for the reference-state ligand bound to the protein for acceleration σ-levels of 2σ (D) and 3σ (E) of system PNMT. Note that in panels A, C, D and E relative free-energy differences $\Delta F_{i\neq1,1}$ falls off the plot.
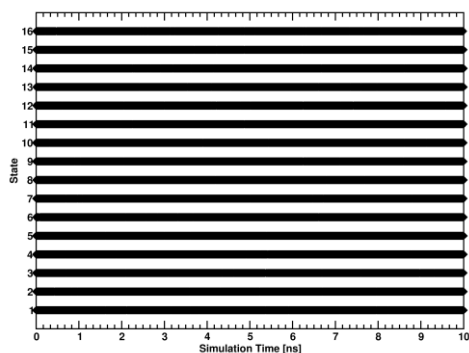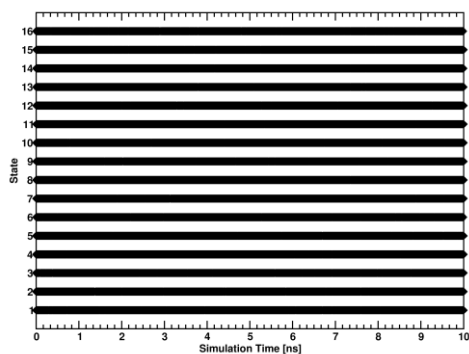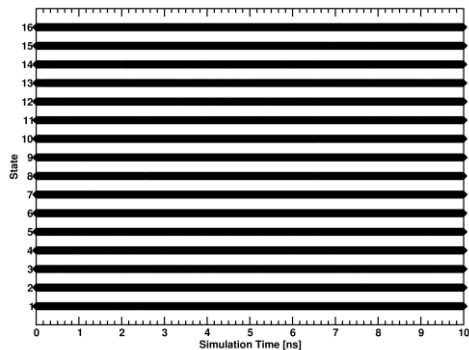
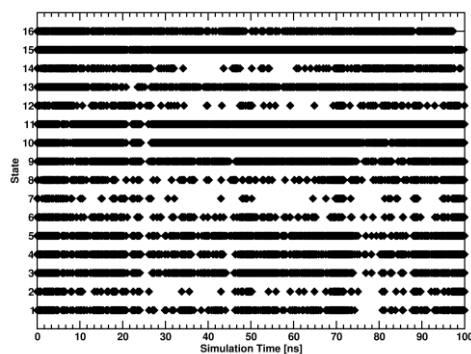**Figure S6.** Ligand end-state timeseries in the equilibrium A-EDS simulations of the unbound reference-state ligand in water for acceleration σ-levels of 1σ (A), 2σ (B) and 3σ (C), and for the reference-state ligand bound to the protein for acceleration σ-levels of 2σ (D) and 3σ (E) of system GRA2. At every timepoint, the state that is currently sampled is marked. Regular exchanges lead to continuous bars, due to the size of the marker.
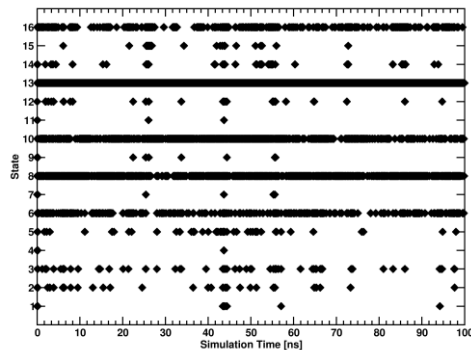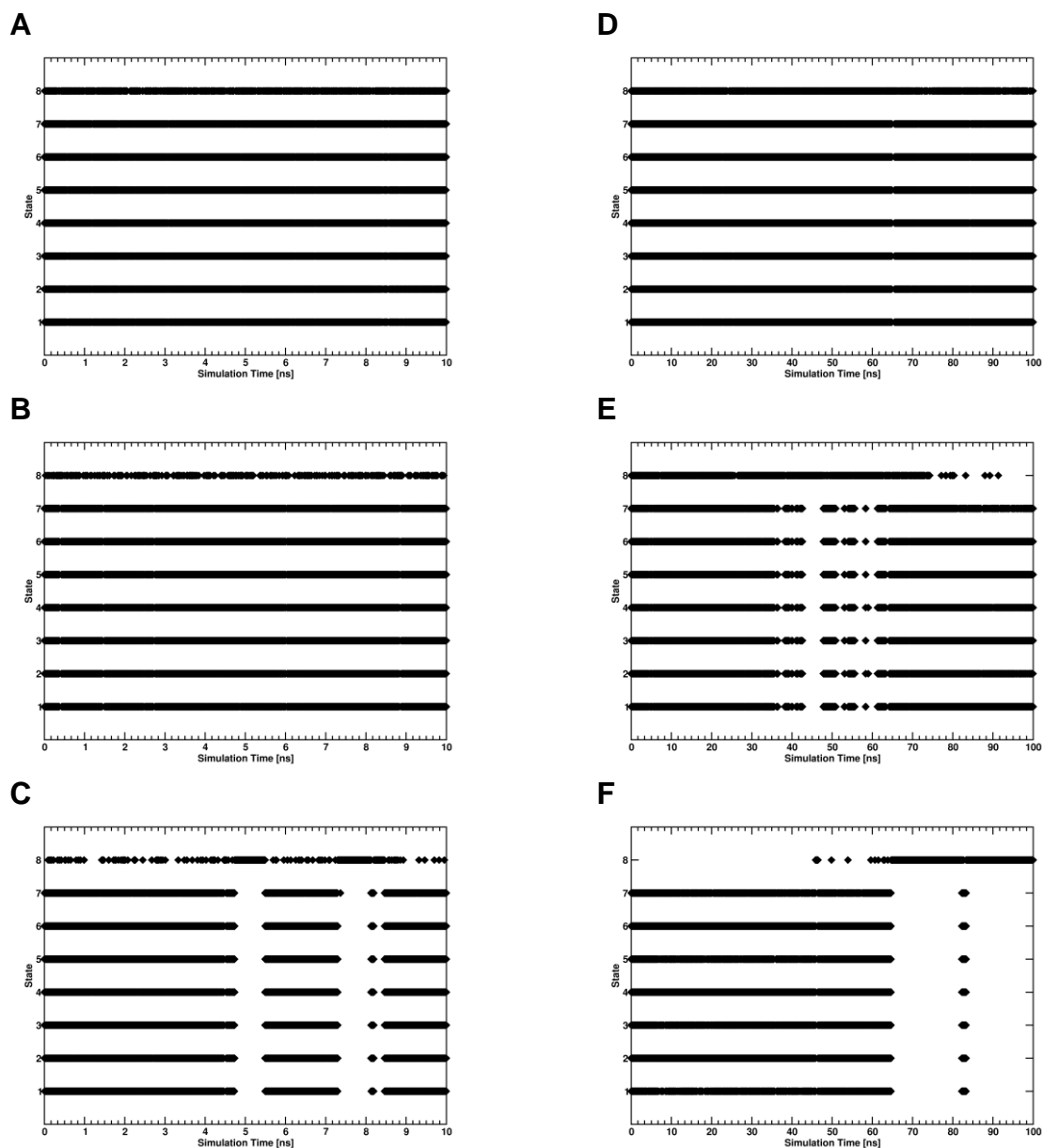
Figure S7. Ligand end-state timeseries in the equilibrium A-EDS simulations of the unbound reference-state ligand in water for acceleration σ-levels of 1σ (A), 2σ (B) and 3σ (C), and for the reference-state ligand bound to the protein for acceleration σ-levels of 1σ (D), 2σ (E) and 3σ (F) of system TRP. At every timepoint, the state that is currently sampled is marked. Regular exchanges lead to continuous bars, due to the size of the marker.
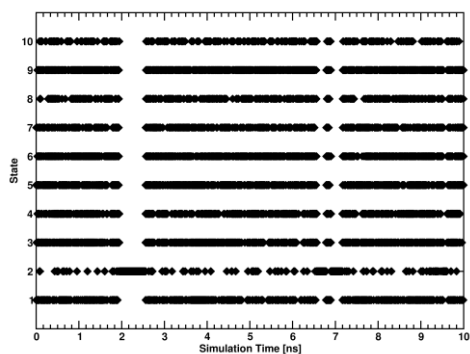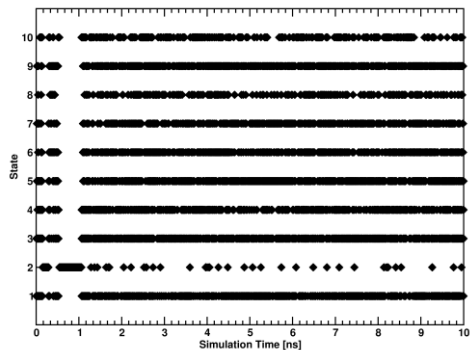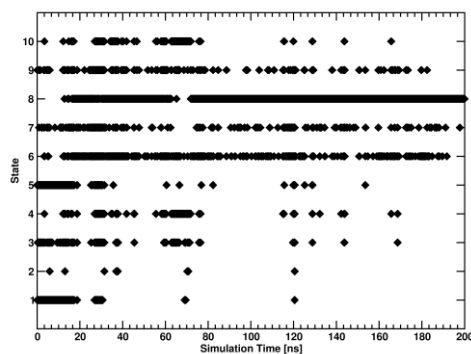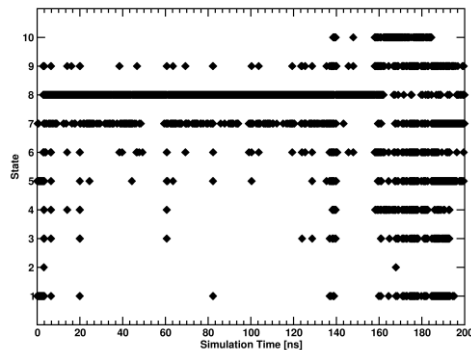
Figure S8. Ligand end-state timeseries in the equilibrium A-EDS simulations of the unbound reference-state ligand in water for acceleration σ-levels of 1σ (A), 2σ (B) and 3σ (C), and for the reference-state ligand bound to the protein for acceleration σ-levels of 2σ (D) and 3σ (E) of system PNMT. At every timepoint, the state that is currently sampled is marked. Regular exchanges lead to continuous bars, due to the size of the marker.
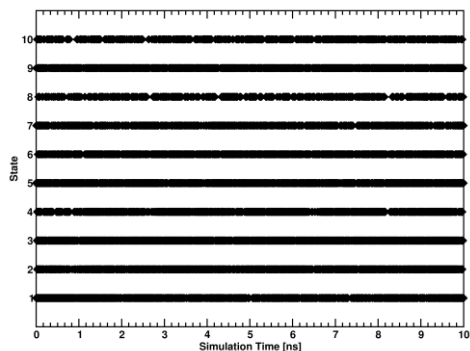
Table S6. Number of transitions between end-states during the first 10 ns of the A-EDS parameter search simulations with the ligand reference state bound to the protein.

Acceleration Level	System GRA2	System TRP	System PNMT
1σ	-	25655	11030
2σ	21331	25210	9979
3σ	17434	20719	4821

Table S7. A-EDS free-energy offset parameter search results for the three different acceleration σ-levels for system GRA2. Energy units are kJ·mol^{-1}.

	Unbound Ligand			Two Bound Ligands		
	1σ	2σ	3σ	1σ	2σ	3σ
ΔF_2^R	-93.1	-100.0	-208.6	-	-189.6	-208.9
ΔF_3^R	38.9	31.9	57.0	-	81.3	74.3
ΔF_4^R	27.0	19.4	30.0	-	20.0	29.6
ΔF_5^R	1.4	-23.2	-74.0	-	-55.6	-72.5
ΔF_6^R	-57.6	-71.1	-157.8	-	-113.9	-142.6
ΔF_7^R	-70.3	-84.5	-185.6	-	-155.3	-179.6
ΔF_8^R	-68.2	-99.2	-232.4	-	-200.5	-235.9
ΔF_9^R	93.9	79.1	142.4	-	161.4	160.6
ΔF_{10}^R	-6.1	-36.9	-107.4	-	-75.7	-101.9
ΔF_{11}^R	20.1	-11.1	-56.6	-	-39.4	-52.9
ΔF_{12}^R	-7.3	-27.7	-78.2	-	-26.7	-63.1
ΔF_{13}^R	-79.1	-115.3	-270.0	-	-231.0	-271.1
ΔF_{14}^R	-53.4	-89.6	-219.2	-	-179.8	-219.3
ΔF_{15}^R	40.3	3.8	-32.0	-	-4.7	-26.5
ΔF_{16}^R	-35.8	-77.1	-199.0	-	-152.3	-194.8

Table S8. A-EDS free-energy offset parameter search results for the three different acceleration σ-levels for system TRP. Energy units are kJ·mol^{-1}.

	Unbound Ligand			Bound Ligand		
	1σ	2σ	3σ	1σ	2σ	3σ
ΔF_2^R	-42.8	-49.1	-54.1	-32.0	-40.0	-12.8
ΔF_3^R	-88.8	-90.4	-91.9	-90.4	-94.2	-77.9
ΔF_4^R	165.4	159.4	155.5	146.4	139.0	178.0
ΔF_5^R	-105.0	-105.8	-107.1	-98.9	-102.0	-87.2
ΔF_6^R	31.9	29.2	26.4	24.7	18.7	54.0
ΔF_7^R	17.1	11.2	6.2	11.5	5.7	34.7
ΔF_8^R	-158.0	-180.5	-198.5	-137.4	-152.8	-161.4

Table S9. A-EDS free-energy offset parameter search results for the three different acceleration σ-levels for system PNMT. Energy units are kJ·mol^{-1}.

	Unbound Ligand			Bound Ligand		
	1σ	2σ	3σ	1σ	2σ	3σ
ΔF_2^R	-50.5	-168.8	-189.8	-	-97.6	-107.2
ΔF_3^R	117.6	81.5	77.0	-	73.1	72.6
ΔF_4^R	178.7	120.7	113.0	-	108.6	117.3
ΔF_5^R	142.6	99.5	94.9	-	79.9	90.9
ΔF_6^R	206.4	131.1	121.5	-	114.7	119.2
ΔF_7^R	-228.0	-297.6	-303.7	-	-297.0	-300.0
ΔF_8^R	-186.9	-285.5	-297.8	-	-291.0	-288.8
ΔF_9^R	207.2	143.5	135.0	-	126.2	132.3
ΔF_{10}^R	55.9	-16.8	-17.4	-	-29.3	-5.8

References

1.   Norholm, A. B.; Francotte, P.; Goffin, E.; Botez, I.; Danober, L.; Lestage, P.; Pirotte, B.; Kastrup, J. S.; Olsen, L.; Oostenbrink, C., Thermodynamic characterization of new positive allosteric modulators binding to the glutamate receptor A2 ligand-binding domain: combining experimental and computational methods unravels differences in driving forces. *J Chem Inf Model* **2014**, 54, 3404-16.

2.   Perthold, J. W.; Oostenbrink, C., Accelerated Enveloping Distribution Sampling: Enabling Sampling of Multiple End States while Preserving Local Energy Minima. *J Phys Chem B* **2018**, 122, 5030-5037.

3.   Mares-Guia, M.; Nelson, D. L.; Rogana, E., Electronic effects in the interaction of para-substituted benzamidines with trypsin: the involvement of the pi-electronic density at the central atom of the substituent in binding. *J Am Chem Soc* **1977**, 99, 2331-6.

4.   de Ruiter, A.; Oostenbrink, C., Efficient and Accurate Free Energy Calculations on Trypsin Inhibitors. *J Chem Theory Comput* **2012**, 8, 3686-95.

5.   Nair, P. C.; Malde, A. K.; Mark, A. E., Using Theory to Reconcile Experiment: The Structural and Thermodynamic Basis of Ligand Recognition by Phenylethanolamine N-Methyltransferase (PNMT). *J Chem Theory Comput* **2011**, 7, 1458-68.

6.   Grunewald, G. L.; Sall, D. J.; Monn, J. A., Synthesis and evaluation of 3-substituted analogues of 1,2,3,4-tetrahydroisoquinoline as inhibitors of phenylethanolamine N-methyltransferase. *J Med Chem* **1988**, 31, 824-30.

7.   Grunewald, G. L.; Dahanukar, V. H.; Teoh, B.; Criscione, K. R., 3,7-Disubstituted-1,2,3,4-tetrahydroisoquinolines display remarkable potency and selectivity as inhibitors of phenylethanolamine N-methyltransferase versus the alpha2-adrenoceptor. *J Med Chem* **1999**, 42, 1982-90.

8.   Wu, Q.; Gee, C. L.; Lin, F.; Tyndall, J. D.; Martin, J. L.; Grunewald, G. L.; McLeish, M. J., Structural, mutagenic, and kinetic analysis of the binding of substrates and inhibitors of human phenylethanolamine N-methyltransferase. *J Med Chem* **2005**, 48, 7243-52.

9.   Grunewald, G. L.; Seim, M. R.; Regier, R. C.; Martin, J. L.; Gee, C. L.; Drinkwater, N.; Criscione, K. R., Comparison of the binding of 3-fluoromethyl-7-sulfonyl-1,2,3,4-tetrahydroisoquinolines with their isosteric sulfonamides to the active site of phenylethanolamine N-methyltransferase. *J Med Chem* **2006**, 49, 5424-33.

10.   Gee, C. L.; Drinkwater, N.; Tyndall, J. D.; Grunewald, G. L.; Wu, Q.; McLeish, M. J.; Martin, J. L., Enzyme adaptation to inhibitor binding: a cryptic binding site in phenylethanolamine N-methyltransferase. *J Med Chem* **2007**, 50, 4845-53.

11.   Riniker, S.; Christ, C. D.; Hansen, N.; Mark, A. E.; Nair, P. C.; van Gunsteren, W. F., Comparison of enveloping distribution sampling and thermodynamic integration to calculate binding free energies of phenylethanolamine N-methyltransferase inhibitors. *J Chem Phys* **2011**, 135, 024105.

12.   Sidler, D.; Cristofol-Clough, M.; Riniker, S., Efficient Round-Trip Time Optimization for Replica-Exchange Enveloping Distribution Sampling (RE-EDS). *J Chem Theory Comput* **2017**, 13, 3020-3030.